

DOX-PLGA Nanoparticles Effectively Suppressed the Expression of Pro-Inflammatory Cytokines TNF- α , IL-6, iNOS, and IL-1 β in MCF-7 Breast Cancer Cell Line

Rawan Hassan AL-Saeedi¹, Mohammad Khalaj-Kondori^{*1},
Mohammad Ali Hosseinpour Feizi¹, Jafar Hajavi^{2,3}

Abstract

Background: Inflammation contributes to cancer pathobiology through different mechanisms. Higher levels of pro-inflammatory cytokines can lead to hyperinflammation and promote cancer development and metastasis. For cancer treatment, Doxorubicin (DOX) can be encapsulated into the poly-lactic-glycolic acid (PLGA) nanoparticles. This study aimed to investigate the impact of doxorubicin-loaded PLGA nanoparticles (DOX-PLGA NP) on the expression of pro-inflammatory genes TNF- α , IL-6, iNOS, and IL-1 β in the MCF-7 cells.

Methods: The DOX-PLGA NP was prepared by loading doxorubicin into PLGA and characterized using dynamic light scattering (DLS) and atomic force microscopy (AFM). The cytotoxic effect of the nanoparticles was determined by the MTT assay, and their impacts on the expression of pro-inflammatory genes were assessed by qRT-PCR.

Results: The encapsulation efficiency and loading capacity were 60 ± 1.5 and 1.13 ± 0.21 percent, respectively. The zeta potential and mean DOX-PLGA nanoparticle size were -18 ± 0.550 mV and 172 ± 55.6 nm, respectively. The 50% inhibitory concentration (IC₅₀) of the DOX-PLGA NP on MCF-7 cell viability was 24.55 μ g/mL after 72 hours of treatment. The qRT-PCR results revealed that the 20 μ g/mL concentration of the DOX-PLGA NP significantly suppressed the expression of the pro-inflammatory genes TNF- α , IL-6, iNOS, and IL-1 β compared to DOX alone (20 μ g/mL). Additionally, the suppression effect of DOX-PLGA NP on the expression of these pro-inflammatory genes was dose-dependent.

Conclusion: These results show that DOX-PLGA NP efficiently suppressed the expression of pro-inflammatory genes. Furthermore, encapsulation of DOX into PLGA nanoparticles significantly improved the effectiveness of DOX in suppressing pro-inflammatory genes in MCF-7 breast cancer cells.

Keywords: Breast cancer, Cytokines, Doxorubicin, Polylactic Acid-Polyglycolic Acid Copolymer, Pro-inflammatory cytokine.

Introduction

Breast cancer, the most prevalent cancer type and a leading cause of mortality in women globally, affects millions annually (1-3). In 2023, the World Health Organization (WHO) reported that with 2.3 million cases annually,

breast cancer is the most frequent type of cancer among adults and about 80% of deaths from breast and cervical cancers occur in low- and middle-income nations (4). In fact, it is the primary or secondary cause of mortality from

1: Department of Animal Biology, Faculty of Natural Sciences, University of Tabriz, Tabriz, Iran.

2: Department of Microbiology, Faculty of Medicine, Infectious Diseases Research Center, Gonabad University of Medical Science, Gonabad, Iran.

3: Innovative Medical Research Center, Mashhad Branch, Islamic Azad University, Mashhad, Iran.

*Corresponding author: Mohammad Khalaj-Kondori; Tel: +98 9123351124; E-mail: khalaj@tabrizu.ac.ir.

Received: 10 Dec, 2023; Accepted: 14 Jun, 2024

cancer in women in 95% of the world's nations, with over 70% of occurrences among women under 70 years of age (5, 6).

Inflammation is a biological response to harmful stimuli, and is associated with different diseases, including cancer (7, 8). Inflammation has both anti- and pro-tumor functions. By acting as an immune response, it activates immune cells and boosts production of the inflammatory proteins to fight cancerous cells (9). On the other hand, it is related to the cancer development, progression, and metastasis (10,11). In the microenvironment of inflammation, neutrophils and macrophages produce reactive nitrogen and reactive oxygen species, which are closely related to the tumorigenesis (8). Besides, some inflammatory factors play roles in the cancer growth and progression (12). Pro-inflammatory cytokines including the tumor necrosis factor alpha (TNF- α), interleukin 6 (IL-6), interleukin 23 (IL-23), and interleukin1-beta (IL-1 β) derived from myeloid-derived suppressive cells (MDSC) or tumor associated macrophages (TAM) are recognized as tumor-promoting cytokines (9, 13). IL-6 promotes activation of the signal transducer and activator of transcription 3 (STAT3), which causes proliferation of cancer cells while inhibiting their apoptosis (14). It also functions as an angiogenic factor (13). In several cancer models, TNF- α plays an important role through the induction of NF- κ B (15). Similar to the TNF- α , the IL-1 β can also activate NF- κ B and its polymorphisms were reported to be linked to gastric cancer (13). It was also reported that induced nitric oxide synthase (iNOS) mediates nitrification of the STAT1 to inhibit IFN- γ signaling (16). The iNOS function leads to the production of nitric oxide (NO), which inhibits the defense mechanisms of tumor cells (16).

Chemotherapy is a widespread form of cancer treatment that employs chemical medications to destroy cancer cells (17, 18). One of the most efficient medications for treating different adult and pediatric cancers is doxorubicin (DOX) (19). Although DOX is one of the most effective chemotherapy drugs, their use is limited due to serious side effects and

toxicity that may occur during or after treatment (20, 21). In this regard, researches are trying to introduce a rather safer and more efficient strategies for application of this common chemotherapy drug for cancer treatment (22, 23). A biodegradable polymer called polylactic-glycolic acid (PLGA) has been widely employed in drug administration, particularly chemotherapy (24). Encapsulation of DOX within PLGA nanoparticles could prevent its degradation, resulting in increased bioavailability and extended-release of the drug (25). This extended-release can improve therapeutic efficacy by maintaining effective drug concentrations for an extended period (26).

This study aimed to compare the effects of DOX-PLGA NPs and free DOX on the expression levels of pro-inflammatory genes *TNF- α* , *IL-6*, *iNOS*, and *IL-1 β* in MCF-7 cells.

Materials and Methods

The human breast cancer cell line, MCF-7, was sourced from the Research Institute of Biotechnology (RIB) at Ferdowsi University of Mashhad. The RPMI 1640 medium, fetal bovine serum, trypsin, and antibiotics were procured from Hyclone (Logan, UT, USA). Additionally, PLGA and dimethyl sulfoxide (DMSO) were purchased from Sigma-Aldrich (France).

Preparation of DOX-PLGA

PLGA-containing DOX nanoparticles (DOX-PLGA NPs) were synthesized utilizing the W1/O/W2 method, a widely employed technique for nanoparticle synthesis. (28). In this method, PVA serves as a stabilizer. Initially, 50 mg of PLGA (50:50) polymer powder was dissolved in a vial containing 12.5 ml of dichloromethane organic solvent. The vial was placed on a magnet mixer. For the primary emulsion (W1/O), 100 μ g of DOX (low-dose) (Doxorubicin: PLGA 1:10) and 300 μ g of DOX (high-dose) in a volume of 300 μ l were added to the vial. The mixture was then subjected to a cold-water bath with a sonicator probe (Hielscher Ultrasonic, Germany) for one minute. To achieve the secondary emulsion

(W1/O/W2), the primary mixture was added drop by drop to the sonicated PVA in a sonicator and cold-water bath for four minutes. The final mixture was placed on a stirrer for two hours (room temperature, under a hood) until the organic solvent vaporized and was eliminated. The NPs were centrifuged at 12000 g for 30 minutes to become separated. After each round, the supernatant was removed, and the sedimentation was suspended in distilled water. This step was repeated three times, and the final sedimentation was suspended in 3 ml of distilled water. After being frozen at -80 °C, the NPs, which were dispersed in the water, were lyophilized.

DOX Loading and Encapsulation Efficiency

The bicinchoninic acid (BCA) assay was employed to determine the encapsulation efficiency (EE%) and loading capacity (LC%) of the NPs. Briefly, one milligram of NPs was dissolved in one milliliter of dichloromethane and left for 30 minutes at 37 °C. The dichloromethane was evaporated using nitrogen, and then the pellet was dissolved in PBS (0.1 M) and centrifuged (15 minutes at 13800 g). Finally, the absorbance of supernatant, which contains Doxorubicin, was assessed at 562 nm. The encapsulation efficiency (EE%) and LC% was calculated using equations;

(%EE) = [(Weight of encapsulated DOX)/Total DOX amount] × 100, and
(%LC) = [Weight of encapsulated DOX in PLGA/ weight of NPs] × 100.

Dynamic light scattering analysis

One milligram of lyophilized powder from the prepared DOX-PLGA NP was dissolved in one milliliter of deionized filtered water. The solution was subjected to a sonicator bath for 15 minutes to achieve homogenization. Subsequently, the size and surface charge of the NPs were assessed through dynamic light scattering (DLS) analysis.

Atomic Force Microscopy (AFM) analysis

For Atomic Force Microscopy (AFM) analysis,

one milligram of lyophilized DOX-PLGA NP was dissolved in one milliliter of deionized water. The solution underwent sonication for 30 minutes in a sonicator bath to achieve a uniform and dispersed particle sample. Subsequently, 25 µL of the obtained uniform sample was deposited on a glass slide, air-dried, and examined by AFM.

Cell toxicity assay

Cell toxicity was assessed using MTT assay. MCF-7 cells (10⁴ cells/well) were cultured in the 96-well plate and incubated overnight. The cells were treated with serial concentrations (0.2, 0.5, 5, 10, 20, 30, and 40 µg/mL) of DOX-PLGA for 72 hours. Subsequently, 20 µL MTT solution was added to each well, and after a 4-hour incubation, the medium was replaced with 100 µL of DMSO. Optical density (OD) was measured at 570 nm using an ELISA reader.

RNA extraction and qRT-PCR

The MCF-7 cells were cultured in six-well plates (2 × 10⁵ cells/well) and incubated overnight. The medium was then replaced with fresh medium, and the cells were treated with 0.0, 0.2, 0.5, 5.0, 10.0, and 20.0 µg/mL of DOX-PLGA for 72 hours. After treatment, the cells were detached by Trypsin-EDTA, the medium was centrifuged, and the cells were collected. Total cell RNA was extracted from the collected cells using the TRIzol reagent, following the manufacturer's instructions. The concentrations of the extracted RNA samples were determined by spectrophotometry using a NanoDrop device. To eliminate any genomic DNA, RNA samples (two µg) were treated with DNase I (Invitrogen). The DNase I-treated RNA samples were then used for cDNA synthesis with the high-capacity cDNA reverse transcription kit, and the cDNA samples were utilized for qRT-PCR with Power Syber Green Master Mix. The primers used are listed in Table 1, with GAPDH serving as an internal control. The volume of each reaction was 10 µl, implemented in duplicate. The relative expression levels of the studied genes were calculated using the delta-delta Ct method.

Table 1. Sequences of the primers used for qRT-PCR reactions.

Name	Accession no.	Forward (5' to 3')	Reverse (5' to 3')
IL-1 β	NM_000576	GGCTTATTACAGTGGCAATG	TAGTGGTGGTCGGAGATT
IL-6	NM_000600	CCTTCGGTCCAGTTGCCTTC	GATGCCGTCGAGGATGTACC
TNF- α	NM_000594	GTAGCCCATGTTGTAGCAAACC	TCTGGTAGGAGACGGCGATG
iNOS	NM_016368	CCAATCGACTGCGTTTGTCC	GATGTCCCAGCCATCGAACA
GAPDH	NM_001357943	CCAATCGACTGCGTTTGTCC	GATGTCCCAGCCATCGAACA

Statistical analysis

The statistical analysis was performed using Sigma Plot 12 (SYSTAT software, Inc., San Jose, CA, USA). Normality of the data was assessed with the Shapiro-Wilk test. Non-normal data were analyzed with the Kruskal-Wallis test. Comparisons between two or more groups were implemented using t-test and one-way ANOVA, respectively. All data were reported as means \pm standard deviations (SD). The P value less than 0.05 was considered statistically significant.

Results

Characterization of the DOX-PLGA nanoparticles

The encapsulation efficiency and loading capacity of DOX by the PLGA NP were $60.0 \pm 1.5\%$ and $1.15 \pm 0.21\%$, respectively. The surface charge of the DOX-PLGA NPs was measured -18.0 ± 0.550 mV by Zeta sizer. The intensity, volume, and number distributions of the DOX-PLGA NPs were analyzed by DLS. The mean particle sizes based on the intensity, volume, and number distributions were 172.3 ± 10.4 nm, 170.4 ± 10.4 nm and 168.6 ± 10.0 nm respectively. The morphology and size of DOX-PLGA NP were further analyzed by an AFM microscope. The DOX-PLGA NPs had spherical shape and exhibited a suitable distribution (Fig. 1).

Toxicity of the DOX-PLGA NP on MCF-7 cells

To determine the toxic effect of DOX-PLGA NP, the MCF-7 cells were treated with a serial concentration including 0.0, 0.2, 0.5, 5, 10, 20, and 30 $\mu\text{g/mL}$ of the DOX-PLGA NP for 72 hours. A dose-dependent toxic effect for DOX-PLGA NP on the MCF-7 cells was observed.

In fact, the toxicity of the nanoparticles was significant at concentrations equal to or higher than 15.63 $\mu\text{g/mL}$, which could be considered the effective dose of the DOX-PLGA NP on the MCF-7 cells. Furthermore, the 50% inhibitory concentration (IC_{50}) of these nanoparticles was determined 24.55 $\mu\text{g/mL}$ (Fig. 2).

DOX-PLGA NP significantly suppressed expression of pro-inflammatory genes

To understand whether DOX-PLGA NP could affect the expression of the pro-inflammatory genes, the MCF-7 cells were treated with the different concentrations of the prepared nanoparticles. The results indicated significant reductions in the expression levels of the *IL-1 β* gene in the cells treated with 5, 10, and 20 $\mu\text{g/mL}$ concentrations of DOX-PLGA NP compared to the non-treated control cells, and the reductions were dose-dependent. Additionally, a significant decrease in the expression of this gene was observed in the cells treated with 20 $\mu\text{g/mL}$ concentration of DOX-PLGA compared to those treated with 20 $\mu\text{g/mL}$ of free DOX ($p=0.0064$) (Fig. 3A).

The results indicated significant reductions in the *IL-6* gene expression in the cells treated with DOX-PLGA at concentrations of 10 and 20 $\mu\text{g/mL}$ compared to the control group (treated with PBS). Furthermore, a decrease in the expression of this gene was observed in cells treated with 20 $\mu\text{g/mL}$ PLGA-DOX compared to those treated with 20 $\mu\text{g/mL}$ free DOX, and the difference was statistically significant ($p=0.007$) Fig. 3B).

The results showed a rather dose-dependent reduction in the expression of *TNF- α* compared to the non-treated cells but, only the

difference between 20 $\mu\text{g/mL}$ DOX-PLGA treated and non-treated groups was statistically significant ($p<0.0001$). Furthermore, although the *TNF- α* expression was decreased in the 20 $\mu\text{g/mL}$ DOX-PLGA treated group compared to the 20 $\mu\text{g/mL}$ free DOX treated group, the difference was not statistically significant ($p=0.088$) (Fig. 3C).

There were significant reductions in *iNOS* gene expression in the cells treated with the DOX-PLGA NP, specifically at concentrations of 10 $\mu\text{g/mL}$ and 20 $\mu\text{g/mL}$, compared to the non-treated control group. Comparison of the *iNOS* expression levels between 20 $\mu\text{g/mL}$ DOX-PLGA NP and 20 $\mu\text{g/mL}$ free DOX treated groups revealed no difference (Fig. 3D).

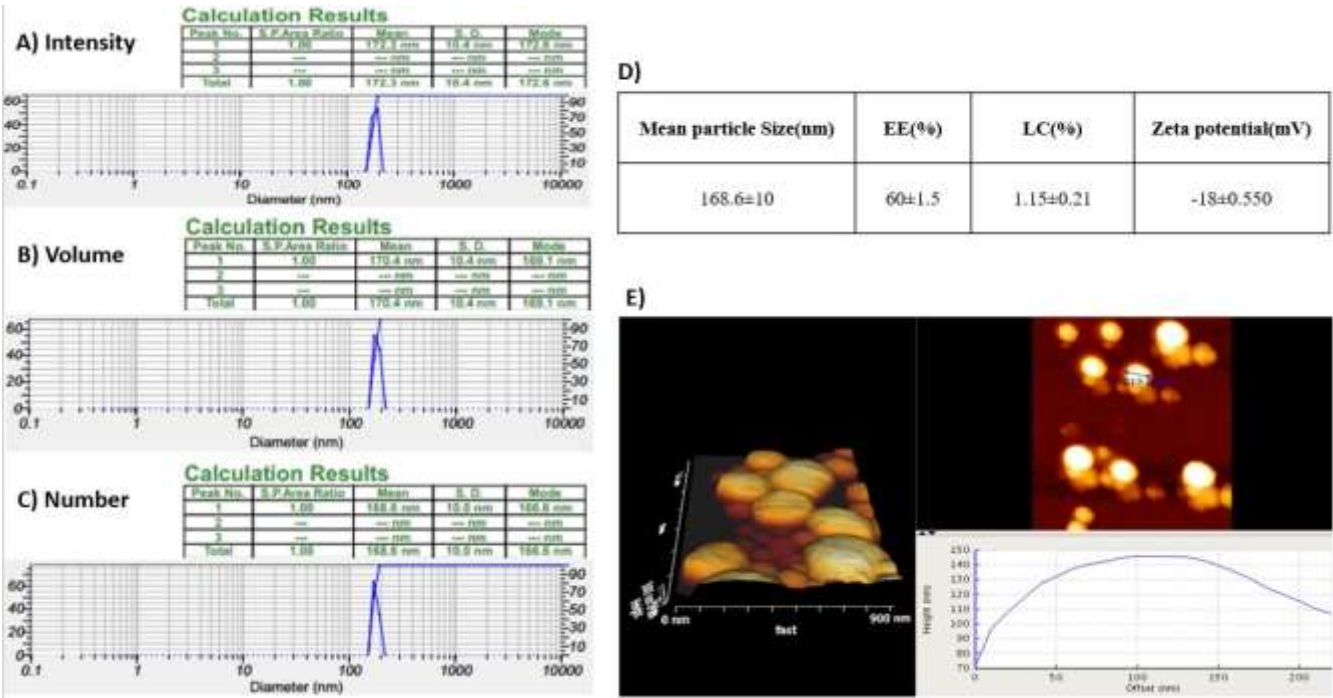


Fig. 1. Characterization of the DOX-PLGA NP by DLS and AFM. A) Intensity distribution, B) Volume distribution, C) Number distribution, and D) a table presenting the mean particle size, encapsulation efficiency (EE%), and loading capacity (LC%) of the DOX-PLGA Nps. E) Pictures captured with AFM showing the spherical shape and size of DOX-PLGA NP.

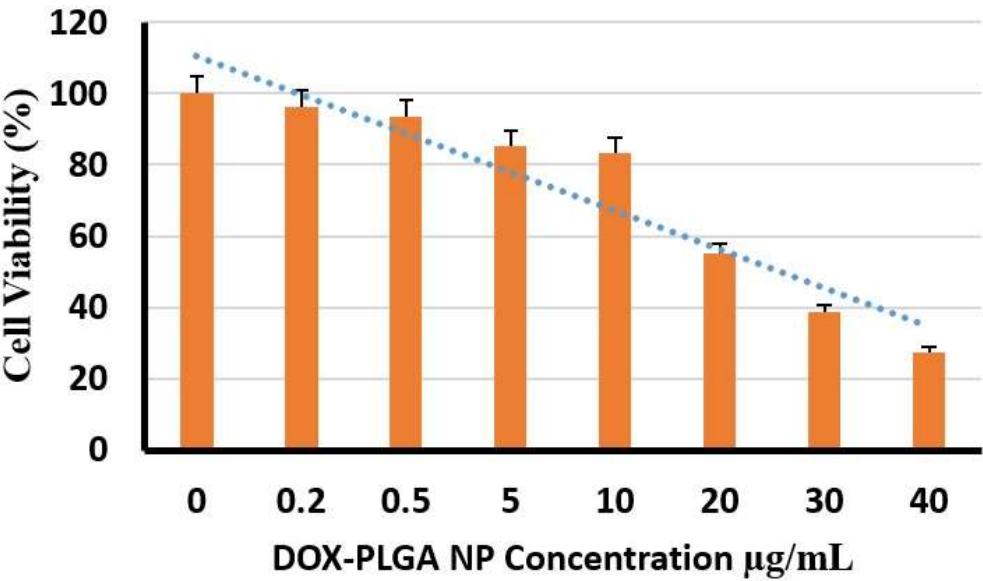


Fig. 2. Toxicity of the DOX-PLGA NP on MCF-7 cells. The cells were treated with different concentrations of the prepared nanoparticle for 72 h and the percent of alive cells was determined.

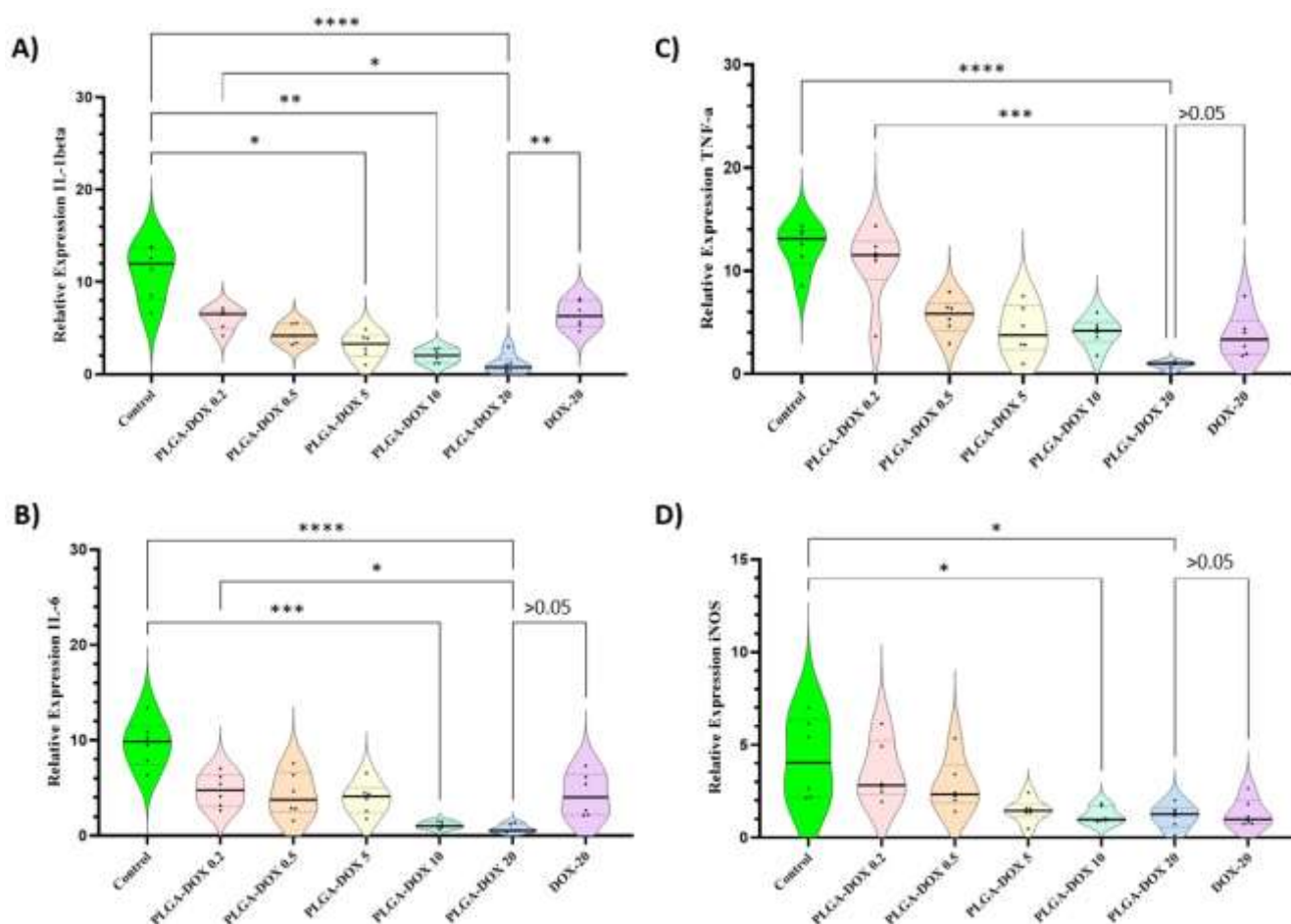


Fig. 3. Effect of the DOX-PLGA NP on the expression levels of pro-inflammatory genes in the MCF-7 cell line. The MCF-7 breast cancer cells were treated with 0.0, 0.2, 0.5, 5.0, 10.0 and 20 µg/mL concentrations of DOX-PLGA NP as well as with a 20 µg/mL concentration of free DOX and the pro-inflammatory genes expression levels including A) *IL-1β*, B) *IL-6*, C) *TNF-α* and D) *iNOS* were quantified with qRT-PCR and compared. * Indicates $P < 0.05$, ** indicates $P < 0.01$, *** indicates $P < 0.001$, and **** indicates $P < 0.0001$.

Discussion

This study showed that treatment of MCF-7 cells with DOX-PLGA NP effectively suppressed expression of the pro-inflammatory cytokines. Characterization of the DOX-PLGA NPs by DLS analysis showed that the mean particle size and mean Zeta potential of the prepared NPs were 168.6 ± 10.0 nm and -18.0 ± 0.550 mV, respectively, which were in line with other reports (27, 28), and suitable for uptake by the cells. Treatment of MCF-7 cells with DOX-PLGA NP showed a dose-dependent toxic effect on the cell viability, and its IC_{50} was obtained 24.55 µg/mL (Fig. 2). These findings are in line with the results of Panda et al. (28) and Kim et al. (27), who reported that DOX-PLGA showed significant cytotoxic effects on the PC-3 and CT26 tumor cells, respectively. Researchers try to improve

the DOX safety by further innovative formulations. As an example, Siddharth et al., encapsulated nanoparticles of the DOX-loaded-PLGA-PVA into the chitosan-dextran sulfate nanoparticles and showed that this formulation was more effective on a derived doxorubicin-resistant MCF-7 cell line (29).

To understand whether DOX-PLGA NP affects the expression of the pro-inflammatory genes, the MCF-7 cells were treated with various concentrations of the DOX-PLGA NP. The results demonstrated a significant dose-dependent reduction in the expression of the *IL-1β* gene (Fig. 3A). Besides, there was a significant difference in the expression level of this gene between the groups treated with 20 µg/mL DOX-PLGA and the DOX alone. This finding implies that loading of DOX into

PLGA can be more effective on the suppression of the *IL-1 β* gene and hence the tumor growth. In fact, it enables reducing the drug dosage significantly while maintaining the same antitumor efficacy, resulting in lower DOX-related adverse effects. Research shows that IL-1 β play a critical role in tumorigenesis by affecting the tumor microenvironment and provoking the initiation and progression of cancer (30). Based on new findings, tumor cells can directly produce IL-1 β in a positive feedback loop, and the cancer patients with higher levels of this cytokine show poor prognosis (30, 31).

Similarly, the results of our study indicated a significant reduction in the expression of the pro-inflammatory *IL-6* gene at the 20 μ g/mL DOX-PLGA concentration compared to the 20 μ g/mL DOX alone. It was reported that IL-6 shows pro-oncogenesis effects in different cancers, such as colorectal, breast, and lung cancers (32, 33). It involves in cancer cell proliferation, angiogenesis and inhibition of apoptosis via activating STAT3 oncoprotein (34).

Based on our findings, the suppressive effect of DOX-PLGA on the *TNF- α* expression was also dose-dependent though the only significant difference was observed between the 20 μ g/mL DOX-PLGA treated and non-treated control groups. Interestingly, loading of DOX into PLGA nanoparticles did not affect the suppressive effect of DOX on the *TNF- α* expression. Studies reported that *TNF- α* shows aberrant expression in several cancers, including liver (35), ovarian (36), prostate (37), and breast (38) cancers. It boosts EMT and cell proliferation, and accelerates angiogenesis by binding to TNF- α R-1 and TNF- α R-2 receptors (39). We also assessed the effect of DOX-PLGA NP on the expression of *iNOS* in the MCF-7 cells. The results revealed a significant reduction in the expression of the *iNOS* gene at 10 μ g/mL DOX- PLGA and 20 μ g/mL DOX- PLGA

concentrations compared to the non-treated control group. Unlikely, the suppressive effect of 20 μ g/mL DOX-PLGA on the expression level of *iNOS* was rather similar to that of 20 μ g/mL DOX alone. Nitric oxide (NO) is a critical pro-inflammatory mediator that is synthesized by iNOS enzyme, and may play important role in cancer development (16). Expression of iNOS is high in many tumors, but its role through development of the tumor might be very complex and confusing, because both inhibiting and promoting effects were described for it (40). In fact, these effects are dependent on the tumor microenvironment. For example, higher levels of iNOS show a positive correlation with tumor degree in some cancers, including gastric cancer, gynecological tumors, hepatocellular carcinoma, squamous cell carcinoma, leukemia, and melanoma (40), while high expression of it is correlated with good prognoses in the lung (41) and ovarian cancers (42).

In conclusion, DOX-PLGA NP effectively decreased expression levels of the pro-inflammatory genes, including *iNOS*, *TNF- α* , *IL-6*, and *IL-1 β* . Furthermore, encapsulation of DOX in PLGA improved its effectiveness on the MCF-7 breast cancer cells, which in turn, might be resulted in decreased adverse effects.

Acknowledgments

The authors appreciate Dr. Mohammad Khakzad for his kind help in preparing DOX-PLGA nanoparticles.

Conflict of interest

The authors declare that there is no conflict of interest.

Funding

No funds, grants, or other support was received.

References

1. Nagarajan D, McArdle SE. Immune landscape of breast cancers. *Biomedicines*. 2018;6(1):20.
2. Karimpur Zahmatkesh A, Khalaj-Kondori M, Hosseinpour Feizi MA, Baradaran B. *GLUL* gene knockdown and restricted glucose level show synergistic inhibitory effect on the luminal subtype breast cancer MCF7 cells' proliferation and metastasis. *EXCLI J*. 2023;22:847-861.
3. Hagag S, Kodous A, Shaaban HA. Molecular and Immunohistochemical Alterations in Breast Cancer Patients in Upper Egypt. *Rep Biochem Mol Biol*. 2023;11(4):532-546.
4. World Health Organization. The Global Breast Cancer Initiative. 3 February 2023. <https://www.who.int/initiatives/global-breast-cancer-initiative>.
5. Budny A, Starosławska E, Budny B. Epidemiologia oraz diagnostyka raka piersi. *Pol Merkuriusz Lek*. 2019;46(275):195-204.
6. Tarighi M, Khalaj-Kondori M, Hosseinzadeh A, Abtin M. Long non-coding RNA (lncRNA) DSCAM-AS1 is upregulated in breast cancer. *Breast Dis*. 2021;40(2):63-8.
7. King TC. Chapter 2, Inflammation, inflammatory mediators, and immune-mediated disease in: . Elsevier's Integrated Pathology. 2007.
8. Balkwill FR, Mantovani A. Cancer-related inflammation: common themes and therapeutic opportunities. *Semin Cancer Biol*. 2012;22(1):33-40.
9. Tahmasebi S, Alimohammadi M, Khorasani S, Rezaei N. Pro-tumorigenic and Anti-tumorigenic Roles of Pro-inflammatory Cytokines in Cancer. In: Rezaei, N. (eds) *Handbook of Cancer and Immunology*. Springer, Cham. 2023.
10. Salem ML, Attia ZI, Galal SM. Acute inflammation induces immunomodulatory effects on myeloid cells associated with anti-tumor responses in a tumor mouse model. *J Adv Res*. 2016;7(2):243-53.
11. Ahangar NK, Hemmat N, Khalaj-Kondori M, Shadbad MA, Sabaie H, Mokhtarzadeh A, Alizadeh N, et al. The Regulatory Cross-Talk between microRNAs and Novel Members of the B7 Family in Human Diseases: A Scoping Review. *Int J Mol Sci*. 2021;22(5):2652.
12. Greten FR, Grivennikov SI. Inflammation and cancer: triggers, mechanisms, and consequences. *Immunity*. 2019;51(1):27-41.
13. Zamarron BF, Chen W. Dual roles of immune cells and their factors in cancer development and progression. *Int J Biol Sci*. 2011;7(5):651-8.
14. Yu H, Pardoll D, Jove R. STATs in cancer inflammation and immunity: a leading role for STAT3. *Nat Rev Cancer*. 2009;9(11):798-809.
15. Karin M. Nuclear factor-kappaB in cancer development and progression. *Nature*. 2006;441(7092):431-6.
16. Xue Q, Yan Y, Zhang R, Xiong H. Regulation of iNOS on Immune Cells and Its Role in Diseases. *Int J Mol Sci*. 2018;19(12):3805.
17. Fisusi FA, Akala EO. Drug Combinations in Breast Cancer Therapy. *Pharm Nanotechnol*. 2019;7(1):3-23.
18. Rahmati-Yamchi M, Zarghami N, Nozad Charoudeh H, Ahmadi Y, Baradaran B, Khalaj-Kondori M, et al. Clofarabine Has Apoptotic Effect on T47D Breast Cancer Cell Line via P53R2 Gene Expression. *Adv Pharm Bull*. 2015;5(4):471-6.
19. Zahedian S, Hekmat A, Tackallou SH, Ghoranneviss M. The Impacts of Prepared Plasma-Activated Medium (PAM) Combined with Doxorubicin on the Viability of MCF-7 Breast Cancer Cells: A New Cancer Treatment Strategy. *Rep Biochem Mol Biol*. 2022;10(4):640-652.
20. Greco G, Ulfo L, Turrini E, Marconi A, Costantini PE, Marforio TD, et al. Light-Enhanced Cytotoxicity of Doxorubicin by Photoactivation. *Cells*. 2023;12(3):392.

21. Kalyanaraman B. Teaching the basics of the mechanism of doxorubicin-induced cardiotoxicity: Have we been barking up the wrong tree? *Redox Biol.* 2020;29:101394.
22. Ahangar NK, Khalaj-Kondori M, Alizadeh N, Mokhtarzadeh A, Baghbanzadeh A, Shadbad MA, Dolatkah K, Baradaran B. Silencing tumor-intrinsic HHLA2 potentiates the anti-tumoral effect of paclitaxel on MG63 cells: Another side of immune checkpoint. *Gene.* 2023;855:147086.
23. Riazi-Tabrizi N, Khalaj-Kondori M, Safaei S, Amini M, Hassanian H, Maghsoudi M, et al. NRF2 Suppression Enhances the Susceptibility of Pancreatic Cancer Cells, Miapaca-2 to Paclitaxel. *Mol Biotechnol.* 2023. <https://doi.org/10.1007/s12033-023-00872-2>.
24. Elmowafy EM, Tiboni M, Soliman ME. Biocompatibility, biodegradation and biomedical applications of poly (lactic acid)/poly (lactic-co-glycolic acid) micro and nanoparticles. *J Pharm Investig.* 2019;49:347-80.
25. Blasi P. Poly (lactic acid)/poly (lactic-co-glycolic acid)-based microparticles: An overview. *J Pharm Investig.* 2019;49:337-46.
26. Hajavi J, Ebrahimian M, Sankian M, Khakzad MR, Hashemi M. Optimization of PLGA formulation containing protein or peptide-based antigen: Recent advances. *J Biomed Mater Res A.* 2018;106(9):2540-2551.
27. Kim J, Choi Y, Yang S, Lee J, Choi J, Moon Y, et al. Sustained and Long-Term Release of Doxorubicin from PLGA Nanoparticles for Eliciting Anti-Tumor Immune Responses. *Pharmaceutics.* 2022;14(3):474.
28. Panda PK, Jain SK. Doxorubicin bearing peptide anchored PEGylated PLGA nanoparticles for the effective delivery to prostate cancer cells. *J Drug Deliv Sci Tech.* 2023;86 (104667).
29. Siddharth S, Nayak A, Nayak D, Bindhani BK, Kundu CN. Chitosan-Dextran sulfate coated doxorubicin loaded PLGA-PVA-nanoparticles caused apoptosis in doxorubicin resistance breast cancer cells through induction of DNA damage. *Sci Rep.* 2017;7(1):2143.
30. Gelfo V, Romaniello D, Mazzeschi M, Sgarzi M, Grilli G, Morselli A, et al. Roles of IL-1 in Cancer: From Tumor Progression to Resistance to Targeted Therapies. *Int J Mol Sci.* 2020;21(17):6009.
31. Bent R, Moll L, Grabbe S, Bros M. Interleukin-1 Beta-A Friend or Foe in Malignancies? *Int J Mol Sci.* 2018;19(8):2155.
32. Heichler C, Scheibe K, Schmied A, Geppert CI, Schmid B, Wirtz S, et al. STAT3 activation through IL-6/IL-11 in cancer-associated fibroblasts promotes colorectal tumour development and correlates with poor prognosis. *Gut.* 2020;69(7):1269-1282.
33. Ke W, Zhang L, Dai Y. The role of IL-6 in immunotherapy of non-small cell lung cancer (NSCLC) with immune-related adverse events (irAEs). *Thorac Cancer.* 2020;11(4):835-839.
34. Bromberg JF, Wrzeszczynska MH, Devgan G, Zhao Y, Pestell RG, Albanese C, Darnell JE Jr. Stat3 as an oncogene. *Cell.* 1999;98(3):295-303.
35. Zhang GP, Yue X, Li SQ. Cathepsin C Interacts with TNF- α /p38 MAPK Signaling Pathway to Promote Proliferation and Metastasis in Hepatocellular Carcinoma. *Cancer Res Treat.* 2020;52(1):10-23.
36. Jo E, Jang HJ, Yang KE, Jang MS, Huh YH, Yoo HS, et al. Cordyceps militaris induces apoptosis in ovarian cancer cells through TNF- α /TNFR1-mediated inhibition of NF- κ B phosphorylation. *BMC Complement Med Ther.* 2020;20(1):1.
37. Schröder SK, Asimakopoulou A, Tillmann S, Koschmieder S, Weiskirchen R. TNF- α controls Lipocalin-2 expression in PC-3 prostate cancer cells. *Cytokine.* 2020;135:155214.
38. Cruceriu D, Baldasici O, Balacescu O, Berindan-Neagoe I. The dual role of tumor necrosis factor-alpha (TNF- α) in breast cancer: molecular insights and therapeutic approaches. *Cell Oncol (Dordr).* 2020;43(1):1-18.
39. Lan T, Chen L, Wei X. Inflammatory

Cytokines in Cancer: Comprehensive Understanding and Clinical Progress in Gene Therapy. *Cells*. 2021;10(1):100.

40. Vannini F, Kashfi K, Nath N. The dual role of iNOS in cancer. *Redox Biol*. 2015;6:334-343.

41. Puhakka A, Kinnula V, Näpänkangas U, Säily M, Koistinen P, Pääkkö P, Soini Y. High

expression of nitric oxide synthases is a favorable prognostic sign in non-small cell lung carcinoma. *APMIS*. 2003;111(12):1137-46.

42. Anttila MA, Voutilainen K, Merivalo S, Saarikoski S, Kosma VM. Prognostic significance of iNOS in epithelial ovarian cancer. *Gynecol Oncol*. 2007;105(1):97-103.